



Cite this: *Phys. Chem. Chem. Phys.*,  
2015, 17, 8276

# Complex transition metal hydrides incorporating ionic hydrogen: thermal decomposition pathway of $\text{Na}_2\text{Mg}_2\text{FeH}_8$ and $\text{Na}_2\text{Mg}_2\text{RuH}_8$

Terry D. Humphries,<sup>\*a</sup> Motoaki Matsuo,<sup>b</sup> Guanqiao Li<sup>a</sup> and Shin-ichi Orimo<sup>ab</sup>

Complex transition metal hydrides have potential technological application as hydrogen storage materials, smart windows and sensors. Recent exploration of these materials has revealed that the incorporation of anionic hydrogen into these systems expands the potential number of viable complexes, while varying the counteranion allows for optimisation of their thermodynamic stability. In this study, the optimised synthesis of  $\text{Na}_2\text{Mg}_2\text{TH}_8$  (T = Fe, Ru) has been achieved and their thermal decomposition properties studied by *ex situ* Powder X-ray Diffraction, Gas Chromatography and Pressure-Composition Isotherm measurements. The temperature and pathway of decomposition of these isostructural compounds differs considerably, with  $\text{Na}_2\text{Mg}_2\text{FeH}_8$  proceeding via  $\text{NaMgH}_3$  in a three-step process, while  $\text{Na}_2\text{Mg}_2\text{RuH}_8$  decomposes via  $\text{Mg}_2\text{RuH}_4$  in a two-step process. The first desorption maxima of  $\text{Na}_2\text{Mg}_2\text{FeH}_8$  occurs at ca. 400 °C, while  $\text{Na}_2\text{Mg}_2\text{RuH}_8$  has its first maxima at 420 °C. The enthalpy and entropy of desorption for  $\text{Na}_2\text{Mg}_2\text{TH}_8$  (T = Fe, Ru) has been established by PCI measurements, with the  $\Delta H_{\text{des}}$  for  $\text{Na}_2\text{Mg}_2\text{FeH}_8$  being 94.5 kJ mol<sup>-1</sup> H<sub>2</sub> and 125 kJ mol<sup>-1</sup> H<sub>2</sub> for  $\text{Na}_2\text{Mg}_2\text{RuH}_8$ .

Received 16th January 2015,  
Accepted 17th February 2015

DOI: 10.1039/c5cp00258c

www.rsc.org/pccp

## Introduction

Transition metals are renowned for their diverse range of valence states and structural conformations.<sup>1,2</sup> As such, in the last five decades a swathe of homoleptic transition metal hydrides have been synthesised to determine their potential for technological applications.  $\text{Mg}_2\text{NiH}_4$  was first realised for its reversible hydrogenation properties in 1968,<sup>3</sup> and has since been investigated for a variety of technological applications including smart windows and sensors.<sup>4–7</sup>  $\text{Mg}_2\text{FeH}_6$ , with a gravimetric hydrogen storage content of 5.5 wt% has since been developed,<sup>8–14</sup> along with a host of other transition metal hydride congeners and derivatives.<sup>1,2,15–22</sup>

The transition metal hydrides of Group 8 often form octahedral  $[\text{TH}_6]^{4-}$  anions, of which are limited to four-fold coordination by counterions (M) in the form of  $\text{M}^+\text{M}'^+\text{M}''^+\text{M}'''^+$ ,  $\text{M}^{2+}\text{M}'^+\text{M}''^+$ ,  $\text{M}^{3+}\text{M}'^+$ ,  $\text{M}^{2+}\text{M}'^{2+}\text{M}''^+$ . Expanding the diversity of coordination can be achieved by increasing the anionic charge of the system, for instance by the inclusion of H<sup>-</sup>. A recent DFT

study by Takagi *et al.* established that the incorporation of anionic hydrogen into complex transition metal hydride compounds enables inclusion of a wider variety of cations, thereby allowing tuning of these materials in order to optimise their thermodynamic properties or hydrogen storage capacities.<sup>23</sup> To date, a variety of quaternary complex hydrides have been synthesised and their structural and physical properties explored, these include  $\text{LaMg}_2\text{NiH}_7$  ( $\text{La}^{3+}\cdot 2\text{Mg}^{2+}\cdot 3\text{H}^-\cdot [\text{NiH}_4]^{4-}$ ),<sup>18,24</sup>  $\text{Na}_2\text{Mg}_2\text{NiH}_6$  ( $2\text{Na}^+\cdot 2\text{Mg}^{2+}\cdot 2\text{H}^-\cdot [\text{NiH}_4]^{4-}$ ),<sup>19,25</sup>  $\text{Na}_2\text{Mg}_2\text{TH}_8$  ( $2\text{Na}^+\cdot 2\text{Mg}^{2+}\cdot 2\text{H}^-\cdot [\text{TH}_6]^{4-}$ ) (T = Fe, Ru),<sup>20</sup>  $\text{MMg}_2\text{FeH}_8$  ( $\text{M}^{2+}\cdot 2\text{Mg}^{2+}\cdot 2\text{H}^-\cdot [\text{TH}_6]^{4-}$ ) (M = Ba, Ca, Sr; T = Fe, Ru, Os)<sup>15,16,26</sup> and  $\text{M}_4\text{Mg}_4\text{Fe}_3\text{H}_{22}$  ( $4\text{Ca}^{2+}\cdot 4\text{Mg}^{2+}\cdot 4\text{H}^-\cdot 3[\text{FeH}_6]^{4-}$ ) (M = Ca, Yb).<sup>27,28</sup> Thermodynamic data for these materials are scarce, although some experimental<sup>15,28</sup> and DFT calculated<sup>23</sup> values have been determined.  $\text{SrMg}_2\text{FeH}_8$  and  $\text{BaMg}_2\text{FeH}_8$  decompose at ca. 440 and 450 °C under 0.1 MPa H<sub>2</sub>,<sup>15</sup> respectively, while  $\text{Ca}_4\text{Mg}_4\text{Fe}_3\text{H}_{22}$  and  $\text{Yb}_4\text{Mg}_4\text{Fe}_3\text{H}_{22}$  decompose at ca. 395 and 420 °C,<sup>1,27,28</sup> respectively. The enthalpy of desorption of  $\text{Ca}_4\text{Mg}_4\text{Fe}_3\text{H}_{22}$  and  $\text{Yb}_4\text{Mg}_4\text{Fe}_3\text{H}_{22}$  to their corresponding binary hydrides has been calculated to be 122 and 137 kJ mol<sup>-1</sup> H<sub>2</sub>, respectively.<sup>28</sup> These values are significantly larger than those determined for the ternary  $\text{Mg}_2\text{FeH}_6$  at 87 kJ mol<sup>-1</sup> H<sub>2</sub>,<sup>29</sup> which decomposes at ca. 300 °C,<sup>13</sup> and indicates the increased stabilisation offered by the incorporation of anionic hydrogen and varied cations into these quaternary compounds.

The isostructural compounds of  $\text{Na}_2\text{Mg}_2\text{FeH}_8$  (5.1 wt% H) and  $\text{Na}_2\text{Mg}_2\text{RuH}_8$  (4.0 wt% H) hold potential as hydrogen

<sup>a</sup> WPI-Advanced Institute for Materials Research, Tohoku University, 2-1-1 Katahira, Aoba-ku, Sendai 980-8577, Japan. E-mail: terry\_humphries81@hotmail.com; Fax: +81-22-215-2091; Tel: +81-22-215-2094

<sup>b</sup> Institute for Materials Research, Tohoku University, 2-1-1 Katahira, Aoba-ku, Sendai 980-8577, Japan. E-mail: orimo@imr.tohoku.ac.jp; Fax: +81-22-215-2091; Tel: +81-22-215-2093



storage materials.<sup>20</sup> To make a fair assumption of their prospective application, a true understanding of the physical properties of these novel quaternary complex transition metal hydrides must be determined, unto which the data is extremely sparse. As a consequence, the influence of  $H^-$  on the thermal stability and decomposition process of these materials is generally unknown and must be understood. As such, *ex situ* powder X-ray diffraction (PXD) and Pressure-Composition Isotherm Measurements (PCI) have been conducted. Their temperatures and pathways of decomposition have been established and the associated enthalpies and entropies of  $H_2$  desorption have been calculated and compared to literature values.

## Experimental

All preparation and manipulation was performed in a Miwa glove box filled with purified argon ( $<1$  ppm  $O_2$  and the dew point of  $H_2O$  below 190 K) to avoid contamination.

The synthesis of  $Na_2Mg_2FeH_8$  was carried out by two methods: S1 followed a four step process, which first required the synthesis of  $Mg_2FeH_6$ . This was achieved by mechanically milling (Fritsch Pulverisette 7)  $MgH_2$  (hydrogen storage grade, Sigma Aldrich) and Fe (99.99%, Mitsuwa) powders at a molar ratio of 2 : 1 for 2 h at 400 rpm (ball-to-powder ratio 40 : 1), under argon with subsequent heat treatment of the pelletised powder at 400 °C for 20 h under 3 MPa  $H_2$ . The resultant olive green powder was then mechanically milled with NaH (95%, Sigma Aldrich) at a molar ratio of 1 : 2 for 20 h under argon (S1-BM) with subsequent heat treatment of the pelletised powder at 400 °C for 20 h under 30 MPa  $H_2$ . The product was yielded as an olive green powder.

The synthesis of S2 ( $Na_2Mg_2FeH_8$ ) followed a two-step process. NaH,  $MgH_2$  and Fe powders at a molar ratio of 2 : 2 : 1 were mechanically milled for 20 h at 400 rpm (ball-to-powder ratio 40 : 1), under argon (S2-BM) with subsequent heat treatment of the pelletised powder at 400 °C for 60 h under 30 MPa  $H_2$ . The product was yielded as an olive green powder.

The synthesis of  $Na_2Mg_2RuH_8$  followed a two-step process.  $MgH_2$ , NaH and Ru (99.9%, Kojundo Chemical Laboratory) were mechanically milled (identical parameters as employed with  $Na_2Mg_2FeH_8$ ) at a molar ratio of 2 : 2 : 1 for 20 h under argon (S3-BM), before subsequent heat treatment of the pelletised powder at 500 °C for 20 h under 30 MPa  $H_2$ . The product was yielded as a light grey powder.

Powder X-ray diffraction (PXD) measurements were conducted using a conventional X-ray diffractometer (Lab-PXD, PANalytical X'Pert-Pro,  $CuK\alpha$  radiation) in flat plate mode. Data were collected using a X'Celerator X linear position sensitive detector within a  $2\theta$  range of 10–90° using 0.02° steps at 0.04°/s with X-ray generator operating conditions of 45 kV and 40 mA. The PXD samples were loaded in an Ar glovebox and the sample holder covered by Mylar film to prevent oxygen/moisture contamination during data collection. PANalytical HighScore Plus v. 3.0, DICVOL,<sup>30</sup> CHEKCELL<sup>31</sup> and GSAS<sup>32,33</sup> were used for phase identification, indexing, space group identification and Rietveld refinement, respectively.

A GC323 (Gas Chromatography) (GL sciences Inc.) was used to detect the desorbed  $H_2$  by means of a TCD detector, with a column temperature of 200 °C. Samples were heated at a rate of 5 °C  $min^{-1}$  under an Ar flow of 40  $ml\ min^{-1}$ .

Typical Pressure-Composition Isotherm Measurements (PCI) were conducted inside custom-built manometric apparatus, where the sample cell was placed in a furnace and heated to the desired temperature at a hydrogen pressure of 6 MPa or 30 MPa. The experiment was controlled by software developed by Suzuki Shokan Co., Ltd.

## Results and discussion

### Synthesis of $Na_2Mg_2TH_8$ (T = Fe, Ru)

The synthesis of  $Na_2Mg_2FeH_8$  was first reported to utilise  $Mg_2FeH_6$  as a starting material, which was consequently milled for 20 h with NaH (S1-BM), followed by hydrogenation at 30 MPa  $H_2$  at 400 °C (eqn (1) and (2)).<sup>20</sup> Overall, this method is time intensive (in excess of 100 h due to the requirement of two milling and two hydrogenation procedures), and the final product also contains Fe, NaH, and  $Mg_2FeH_6$  impurities. In order to reduce the time requirements and levels of impurities, alternative synthetic routes were investigated. It was determined that successful synthesis is achievable by ball milling  $2NaH + MgH_2 + Fe$  (S2-BM), followed by hydrogenation at 30 MPa  $H_2$  at 400 °C (eqn (3)), with an associated time requirement of 80 h. The products after milling of each material differ considerably (Fig. 1), the constituents of S1-BM, identified by PXD are not altered during milling ( $Mg_2FeH_6 + NaH$ ) despite a broadening of the peaks due to a decrease of crystallite size (or reduced crystallinity).<sup>34</sup> The products of S2-BM were  $NaMgH_3 + Fe$ .<sup>35</sup>

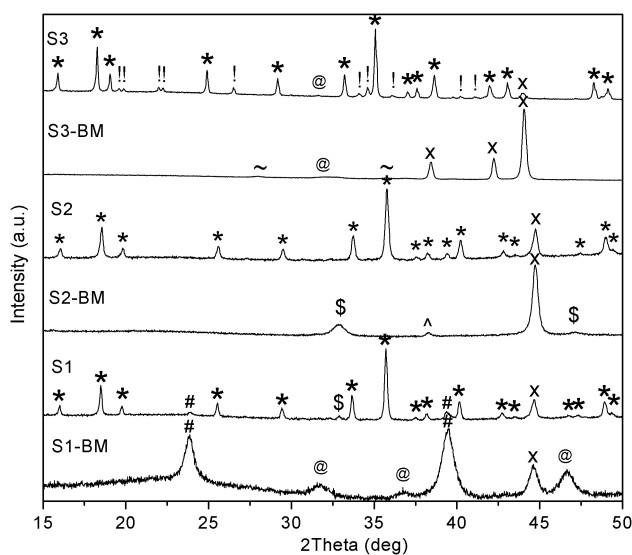


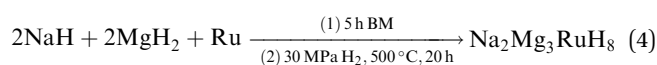
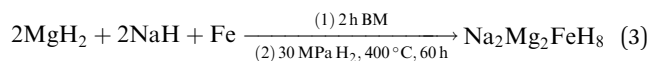
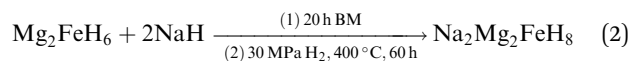
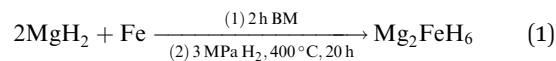
Fig. 1 PXD of ball milled samples S1-BM ( $Mg_2FeH_6 + 2NaH$ ), S2-BM ( $2NaH + 2MgH_2 + Fe$ ) and S3-BM ( $2MgH_2 + 2NaH + Ru$ ) and hydrogenated samples of S1-3.  $\lambda = CuK\alpha$ . \* =  $Na_2Mg_2TH_8$  (T = Fe, Ru); # =  $Mg_2FeH_6$ ; @ = NaH; x = T (Fe, Ru); \$ =  $NaMgH_3$ ; ^ = NaOH; + = Mg; ~ =  $MgH_2$ ; ! = unknown phase.



Hydrogenation of the ball milled samples S1-BM and S2-BM under standard conditions (30 MPa H<sub>2</sub> and 400 °C for 60 h), resulted in the formation of Na<sub>2</sub>Mg<sub>2</sub>FeH<sub>8</sub> as the major phase (Fig. 1). Analysis of hydrogenated S1 by Reitveld refinement indicates that the sample is 80.3(9)% pure and as such contains residual Mg<sub>2</sub>FeH<sub>6</sub> (8.9(4)%), Fe (7.9(2)%), NaMgH<sub>3</sub> (2.5(3)%) and NaH (2.7(2)%) starting materials. Analysis of hydrogenated S2 indicates that the sample contains 90.6(4)% Na<sub>2</sub>Mg<sub>2</sub>FeH<sub>8</sub> and 9.4(3)% Fe, without residual Mg<sub>2</sub>FeH<sub>6</sub> or NaH. This indicates that the optimal method of synthesis is *via* the S2 method due to the elimination of the prerequisite Mg<sub>2</sub>FeH<sub>6</sub> synthesis (eqn (1)) and overall decrease in impurities compared to S1, primarily due to the initial (complete) formation of NaMgH<sub>3</sub> during the milling reaction. Milling initiates the breaking of the strong Na–H bonds, which is required to ensue during the annealing phase when synthesised *via* Mg<sub>2</sub>FeH<sub>6</sub> (S1). This ultimately leads to the observation of unreacted NaH and Mg<sub>2</sub>FeH<sub>6</sub> starting materials.

The synthesis of Na<sub>2</sub>Mg<sub>2</sub>RuH<sub>8</sub> follows a two-step reaction, where stoichiometric quantities of Ru, NaH and MgH<sub>2</sub> are milled for 5 h (S3-BM) before hydrogenation under 30 MPa H<sub>2</sub> at 500 °C for 20 h (S3) (eqn (4)).<sup>20</sup> The composition of the milled material is unchanged from the starting materials

(Fig. 1), whereas after hydrogenation the sample appears to be mostly Na<sub>2</sub>Mg<sub>2</sub>RuH<sub>8</sub>, but also comprises of some residual Ru. An unknown material is also identifiable within the Na<sub>2</sub>Mg<sub>2</sub>RuH<sub>8</sub> powder (S3), of which only a few reflections are discernible. The occurrence of these additional Bragg peaks were also noted previously.<sup>20</sup>



### Thermal decomposition of Na<sub>2</sub>Mg<sub>2</sub>TH<sub>8</sub> (T = Fe, Ru)

In order to determine the thermal decomposition temperatures of Na<sub>2</sub>Mg<sub>2</sub>TH<sub>8</sub> (T = Fe, Ru), aliquots of each material were heated at a rate of 5 °C min<sup>−1</sup> with GC detecting the corresponding desorbed H<sub>2</sub>. The chromatograms obtained (Fig. 2a)

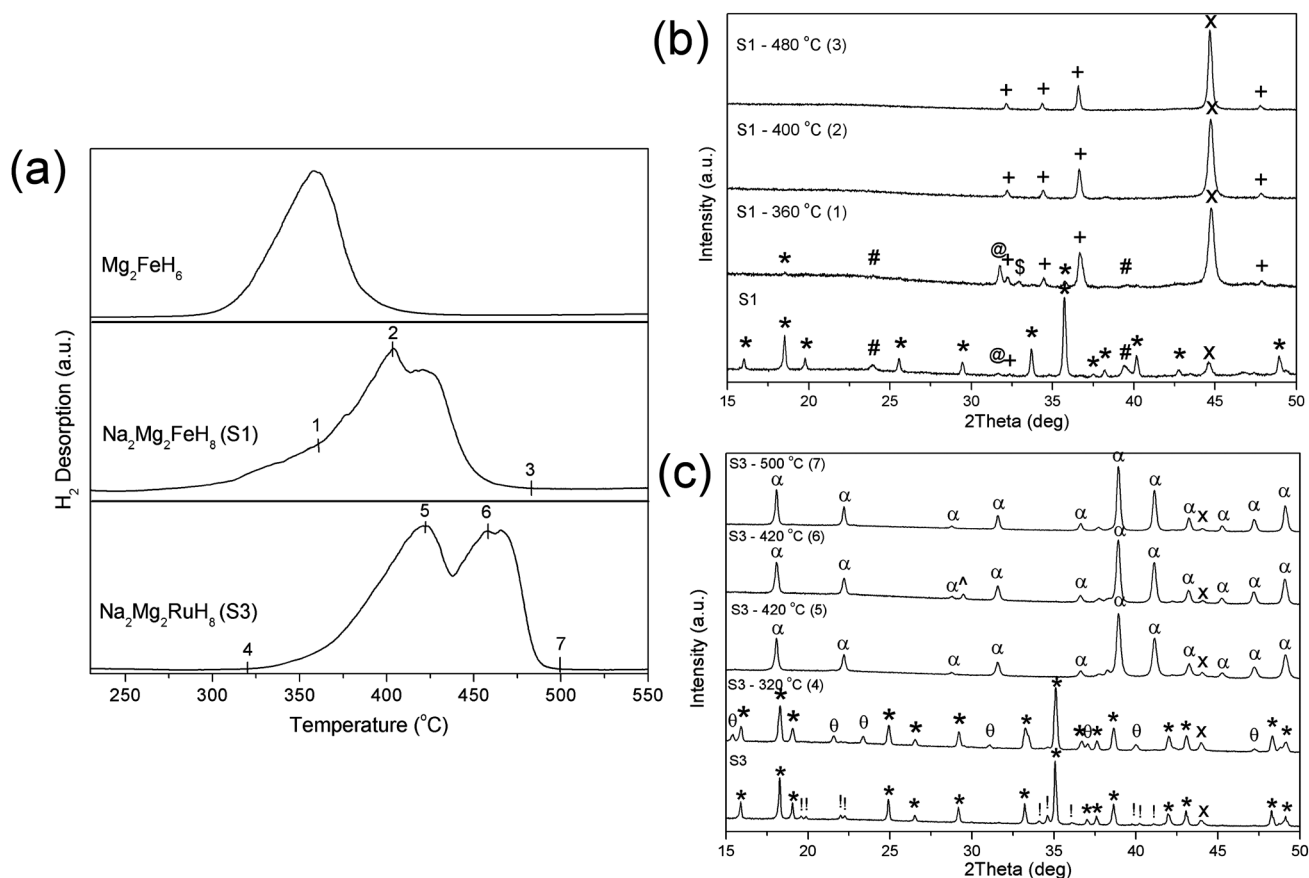
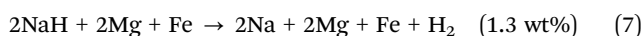
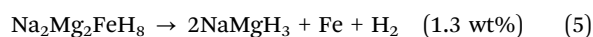


**Fig. 2** (a) GC analysis of Mg<sub>2</sub>FeH<sub>6</sub>, Na<sub>2</sub>Mg<sub>2</sub>FeH<sub>8</sub> (S1) and Na<sub>2</sub>Mg<sub>2</sub>RuH<sub>8</sub> (S3) ( $\Delta T = 5^\circ\text{C min}^{-1}$ ). *Ex situ* PXD analysis of (b) Na<sub>2</sub>Mg<sub>2</sub>FeH<sub>8</sub> (S1) and (c) Na<sub>2</sub>Mg<sub>2</sub>RuH<sub>8</sub> (S3) at selected temperatures ( $\lambda = \text{CuK}\alpha$ ). Numbers on GC plots correlate to temperatures at which samples were heated prior to PXD analysis. \* = Na<sub>2</sub>Mg<sub>2</sub>TH<sub>8</sub> (T = Fe, Ru); # = Mg<sub>2</sub>FeH<sub>6</sub>; @ = NaH; x = T (Fe, Ru); \$ = NaMgH<sub>3</sub>; ^ = NaOH; + = Mg; α = Mg<sub>3</sub>Ru<sub>2</sub>; ! = unknown phase; θ = unknown phase.

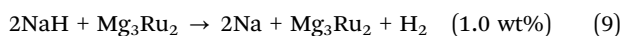


are similar, with two stages of H<sub>2</sub> desorption being observed for both materials (S1 and S3). The onset of decomposition for Na<sub>2</sub>Mg<sub>2</sub>FeH<sub>8</sub> occurs at *ca.* 280 °C, with the first maxima being observed at *ca.* 400 °C, and the second at *ca.* 430 °C. Decomposition concludes at *ca.* 475 °C. Conversely, the onset of H<sub>2</sub> desorption for Na<sub>2</sub>Mg<sub>2</sub>RuH<sub>8</sub> occurs at *ca.* 325 °C, with the first maxima being observed at *ca.* 421 °C, and the second at *ca.* 460 °C. H<sub>2</sub> is no longer detected after *ca.* 500 °C.

To ascertain the pathway of decomposition, *ex situ* PXD was conducted on samples heated to selected temperatures *in vacuo* (Fig. 2b and c). Analysis of Na<sub>2</sub>Mg<sub>2</sub>FeH<sub>8</sub> after heating at 360 °C indicates a miniscule quantity of Na<sub>2</sub>Mg<sub>2</sub>FeH<sub>8</sub> resides, although the majority has decomposed into NaH, Mg and Fe, while NaMgH<sub>3</sub> is also detected. By 400 °C NaH has decomposed, while only Mg and Fe are observable by PXD. Na is not observed due to the low vapor pressure of Na at elevated temperatures. No further changes to the material are observed at higher temperatures. Therefore the decomposition of Na<sub>2</sub>Mg<sub>2</sub>FeH<sub>8</sub> is determined to occur according to eqn (5)–(7).



Na<sub>2</sub>Mg<sub>2</sub>RuH<sub>8</sub> was first heated to 320 °C, where PXD determined that decomposition has not yet started. By 420 °C full decomposition appears to be complete, with Mg<sub>3</sub>Ru<sub>2</sub> and Ru being the products. At this temperature, NaH instantly decomposes to Na and evaporates from the sample. As a result, the decomposition of Na<sub>2</sub>Mg<sub>2</sub>RuH<sub>8</sub> is determined to occur according to eqn (8) and (9). Presumably the excess Ru required to form Mg<sub>3</sub>Ru<sub>2</sub> (without leaving excess Mg) comes from the excess Ru that remained in the starting material.



PCI analysis of Na<sub>2</sub>Mg<sub>2</sub>TH<sub>8</sub> (T = Fe, Ru) (Fig. 3a and b) enables the intricacies of the decomposition process to be truly understood. The experiments on Na<sub>2</sub>Mg<sub>2</sub>FeH<sub>8</sub> were conducted at initial pressures of 30 MPa and 400 °C, mimicking conditions used for synthesis. Consequently, it was ascertained that the first thermal reaction according to eqn (5), occurs at an equilibrium pressure of 15.5 MPa, releasing *ca.* 0.8 wt% H<sub>2</sub> at 400 °C (Fig. 4a). PXD analysis of the products recovered at 6 MPa characterised the products to be NaMgH<sub>3</sub> and Fe (Fig. 3e).  $\Delta H_{\text{dec}}$  for this process was determined by means of a van't Hoff plot of H<sub>2</sub> desorption equilibrium pressures and the linear fit ( $R^2 = 0.975$ ) to the data to be 93 kJ mol<sup>−1</sup> H<sub>2</sub> (Fig. 3c), while the corresponding  $\Delta S_{\text{dec}}$  was calculated as 180 J mol<sup>−1</sup> H<sub>2</sub>/K. However, at lower temperatures this step is kinetically hindered and as a result  $\Delta H$  and  $\Delta S$  may be obscured. The values reported above are an average of the plateau pressures.

The further two equilibrium plateaus below 1 MPa H<sub>2</sub> correspond to the decomposition of NaMgH<sub>3</sub>, exhibiting mass losses of 2.5 and 1.5 wt% for eqn (6) and (7), respectively. The overall

hydrogen content released was therefore determined to be 4.7 wt% at 400 °C (theoretical maximum of 5.1 wt%).  $\Delta H_{\text{dec}}$  was calculated to be 87 and 111 kJ mol<sup>−1</sup> H<sub>2</sub> for the latter two processes, in accord with the literature values.<sup>36</sup> The corresponding  $\Delta S_{\text{dec}}$  also agreed with literature values with 132 and 158 J mol<sup>−1</sup> H<sub>2</sub>/K for eqn (6) and (7), respectively. Therefore  $\Delta H_{\text{des}}$  for the entire system is surmised to be 378 kJ mol<sup>−1</sup> (94.5 kJ mol<sup>−1</sup> H<sub>2</sub>). The identity of the species at each decomposition stage was determined by PXD by ending selected PCI experiments at specified pressures. Fig. 3e illustrates the final products after the PCI experiments conducted at 360 and 400 °C and also those observed after the first and during the second equilibrium step (eqn (6)). During the second equilibrium step, NaMgH<sub>3</sub>, Fe and NaH, and Mg are observed, indicating that NaMgH<sub>3</sub> is decomposing. After the third equilibrium (final products), Na, Mg and Fe are the main constituents, although residual NaH is also observed. Therefore the decomposition process can be described according to eqn (5)–(7) and Fig. 4.

The thermal stability of Na<sub>2</sub>Mg<sub>2</sub>FeH<sub>8</sub> is enhanced compared to that of Mg<sub>2</sub>FeH<sub>6</sub>, which exhibits a H<sub>2</sub> desorption maxima at *ca.* 360 °C (Fig. 2) with an associated  $\Delta H_{\text{des}}$  of 261 kJ mol<sup>−1</sup>.<sup>29</sup> The additional stability achieved by the incorporation of Na<sup>+</sup> and H<sup>−</sup> into the compound, induces a significant increase in desorption temperature maxima to 400 °C and a total  $\Delta H_{\text{des}}$  of 378 kJ mol<sup>−1</sup> (Fig. 4). This value correlates very well with the previous DFT calculations conducted on this compound, which determined  $\Delta H_f$  to be −328 kJ mol<sup>−1</sup>.<sup>23</sup>

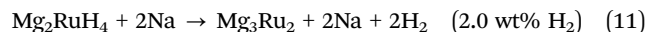
In contrast to Na<sub>2</sub>Mg<sub>2</sub>FeH<sub>8</sub>, Na<sub>2</sub>Mg<sub>2</sub>RuH<sub>8</sub> is stable above pressures of 0.19 MPa H<sub>2</sub> and  $T > 500$  °C (Fig. 3a). PXD analysis of material annealed at 6 MPa H<sub>2</sub> and 450 °C (Fig. 3f) indicates that the only modification is the disappearance of the unknown phase (observed after initial synthesis (Fig. 1)) which is replaced by another unknown phase. This material can be indexed to an orthorhombic unit cell of  $a = 14.5331$ ,  $b = 7.9841$  and  $c = 6.2429$  and crystallises in a possible space group of *Pmmn*, although structural identification is inhibited by the low concentration and weak intensity of the Bragg peaks. As was observed from the GC results (Fig. 1), decomposition is also noted to follow a two-step decomposition route by PCI. At 500 °C, the first plateau is observed at an equilibrium pressure of 0.19 MPa, while the second occurs at *ca.* 0.07 MPa. Each step was determined to have an associated mass loss of *ca.* 1.9 wt%, with a total of 3.8 wt% H<sub>2</sub> being desorbed out of a maximum theoretical capacity of 4.0 wt%. This process was also carried out at 475 and 450 °C. This allowed for  $\Delta H_{\text{des}}$  and  $\Delta S$  to be determined to be 131 kJ mol<sup>−1</sup> H<sub>2</sub> and 176  $\Delta S$  (J mol<sup>−1</sup> H<sub>2</sub>/K), respectively for step 1 ( $R^2 = 0.984$ ) and  $\Delta H_{\text{des}} = 119$  kJ mol<sup>−1</sup> H<sub>2</sub> and  $\Delta S = 151$   $\Delta S$  (J mol<sup>−1</sup> H<sub>2</sub>/K) for step 2 ( $R^2 = 0.999$ ) (Fig. 3d). Therefore  $\Delta H_{\text{des}}$  for the entire system is surmised to be 500 kJ mol<sup>−1</sup> (125 kJ mol<sup>−1</sup> H<sub>2</sub>). PXD of the products at each stage allows a greater insight into those determined by *ex situ* heating *in vacuo*. After the first plateau, a substantial level of Mg<sub>2</sub>RuH<sub>4</sub> is identifiable in the powder, along with Ru, NaOH and a small quantity of Mg<sub>3</sub>Ru<sub>2</sub>. The highly oxidisable Na (residual after evaporation) is the source of NaOH (occurring during PXD analysis),





while the thermally unstable  $\text{Mg}_2\text{RuH}_4$  is the source of  $\text{Mg}_3\text{Ru}_2$ . An unknown phase is also observed at this temperature and pressure, which due to the low intensity of the Bragg peaks associated with this material, indexing and as such, structural refinement was not possible. After the second plateau, the remaining powder consists of  $\text{Mg}_3\text{Ru}_2$  and Ru. Presumably the excess Ru required to form  $\text{Mg}_3\text{Ru}_2$  (without leaving excess Mg) comes from the excess Ru that remains in the starting

material (Fig. 1). Therefore the decomposition process can be described according to eqn (10) and (11) and Fig. 4.



The decomposition pathway of these materials differ significantly in that  $\text{NaMgH}_3$  is the intermediate for  $\text{Na}_2\text{Mg}_2\text{FeH}_8$ ,

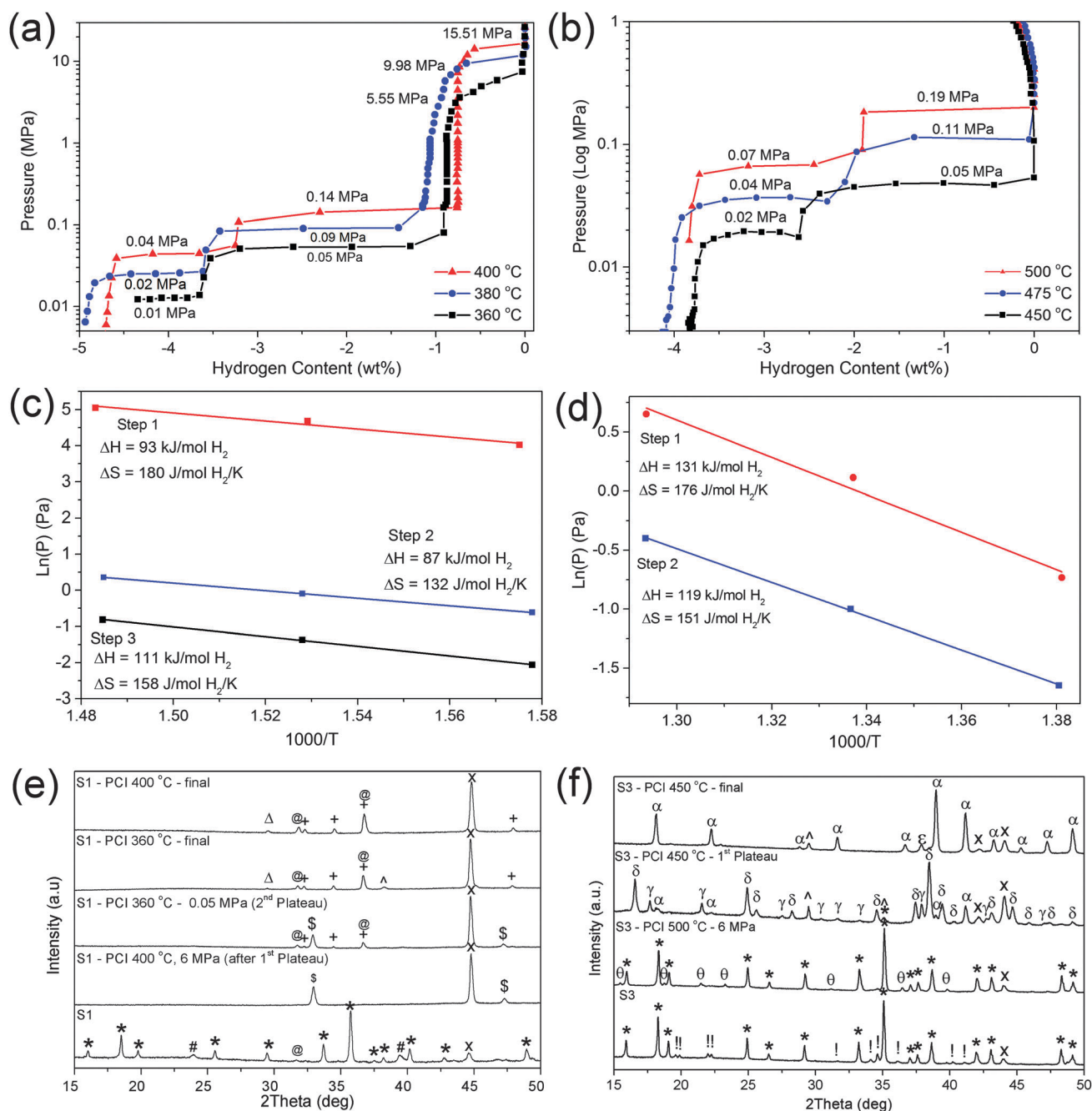


**Fig. 3** PCI analysis of  $\text{Na}_2\text{Mg}_2\text{FeH}_8$  (a) and  $\text{Na}_2\text{Mg}_2\text{RuH}_8$  (b) at selected temperatures. van't Hoff plot of  $\text{H}_2$  desorption equilibrium pressures and the linear fit to the data for  $\text{Na}_2\text{Mg}_2\text{FeH}_8$  (c) and  $\text{Na}_2\text{Mg}_2\text{RuH}_8$  (d). *Ex situ* PXD analysis of  $\text{Na}_2\text{Mg}_2\text{FeH}_8$  (S1) (e) and  $\text{Na}_2\text{Mg}_2\text{RuH}_8$  (S3) (f) for samples collected after PCI analysis and after rehydrogenation ( $\lambda = \text{CuK}\alpha$ ). \* =  $\text{Na}_2\text{Mg}_2\text{TH}_8$  (T = Fe, Ru); # =  $\text{Mg}_2\text{FeH}_6$ ; @ = NaH; x = T (Fe, Ru); \$ =  $\text{NaMgH}_3$ ; ^ = NaOH; + = Mg; Δ = Na; α =  $\text{Mg}_3\text{Ru}_2$ ; δ =  $\text{Mg}_2\text{RuH}_4$ ; ! = unknown phase; θ = unknown phase; γ = unknown phase; ε = unknown phase.

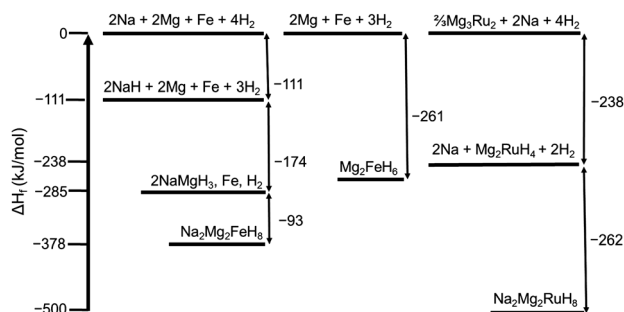


Fig. 4 Energy diagram illustrating the experimentally determined enthalpies of formation ( $\Delta H_{\text{form}}$ ,  $\text{kJ mol}^{-1}$ ) of  $\text{Na}_2\text{Mg}_2\text{FeH}_8$ ,  $\text{Mg}_2\text{FeH}_6$ ,<sup>29</sup> and  $\text{Na}_2\text{Mg}_2\text{RuH}_8$ . The excess Ru required to form  $\text{Mg}_3\text{Ru}_2$  is acquired from the impurity Ru remaining in the  $\text{Na}_2\text{Mg}_2\text{RuH}_8$  starting material.

while  $\text{Na}_2\text{Mg}_2\text{RuH}_8$  disassembles *via*  $\text{Mg}_2\text{RuH}_4$  (Fig. 4). The versatile 4d Ru metal center is known to form a variety of complex anions including  $[\text{Ru}_2\text{H}_6]^{12-}$ ,  $[\text{RuH}_4]_n^{4n-}$ ,  $[\text{RuH}_5]_{\text{av}}^{5-}$ ,  $[\text{RuH}_6]^{4-}$  and  $[\text{RuH}_7]^{3-}$ , while the 3d Fe metal center is only known to form  $[\text{FeH}_6]^{4-}$  anions.<sup>1</sup> As a consequence,  $\text{Na}_2\text{Mg}_2\text{RuH}_8$  forms the  $[\text{RuH}_4]_n^{4n-}$  polyanionic intermediate upon decomposition,<sup>37</sup> whereas  $\text{Na}_2\text{Mg}_2\text{FeH}_8$  preferentially decomposes to the thermally stable  $\text{NaMgH}_3$ <sup>36</sup> rather than  $\text{Mg}_2\text{FeH}_6$  (Fig. 4).  $\text{Mg}_2\text{RuH}_4$  was not observed during the *ex situ* heating experiments of  $\text{Na}_2\text{Mg}_2\text{RuH}_8$  (Fig. 2e) as it is not thermodynamically stable at the temperatures at which  $\text{Na}_2\text{Mg}_2\text{RuH}_8$  decomposes ( $420^\circ\text{C}$ , *in vacuo*).<sup>37</sup> Although, the synthesis of  $\text{Mg}_2\text{RuH}_4$  is accomplished at  $450^\circ\text{C}$  under 0.2 MPa  $\text{H}_2$ , it would presumably decompose at the temperatures imposed here, especially *in vacuo*. Stabilisation of this species is therefore viable under  $\text{H}_2$  pressures of 0.05–0.02 MPa.

## Conclusions

The optimised syntheses of  $\text{Na}_2\text{Mg}_2\text{TH}_8$  (T = Fe, Ru) have been reported. Ball milling of stoichiometric quantities of NaH,  $\text{MgH}_2$  and Fe followed by hydrogenation allows for a yield of >90% purity of  $\text{Na}_2\text{Mg}_2\text{FeH}_8$  *via* the formation of a  $\text{NaMgH}_3$  intermediate. On the contrary, no intermediate is observed during the synthesis of  $\text{Na}_2\text{Mg}_2\text{RuH}_8$  using an identical procedure.

The thermal decomposition of both  $\text{Na}_2\text{Mg}_2\text{TH}_8$  materials have been studied by *ex situ* PXD, GC and PCI measurements. The first desorption maxima of  $\text{Na}_2\text{Mg}_2\text{FeH}_8$  has been established to occur at *ca.*  $400^\circ\text{C}$ , while  $\text{Na}_2\text{Mg}_2\text{RuH}_8$  has its first maxima at  $420^\circ\text{C}$ . The decomposition pathways of these isostructural compounds differs considerably, with  $\text{Na}_2\text{Mg}_2\text{FeH}_8$  proceeding *via*  $\text{NaMgH}_3$  in a three-step process, while  $\text{Na}_2\text{Mg}_2\text{RuH}_8$  decomposes *via*  $\text{Mg}_2\text{RuH}_4$  in a two-step process. The dissimilarity between the pathways originates from the capability of the 4d Ru metal centre to exist in a variety of  $[\text{RuH}_x]^{7-}$  complexes compared to Fe, which only exists as  $[\text{FeH}_6]^{4-}$ .

The enthalpy and entropy of desorption for  $\text{Na}_2\text{Mg}_2\text{TH}_8$  (T = Fe, Ru) for each stage of decomposition has been established to be by PCI measurements. The total enthalpy of desorption for

$\text{Na}_2\text{Mg}_2\text{FeH}_8$  is  $95 \text{ kJ mol}^{-1} \text{H}_2$  and  $125 \text{ kJ mol}^{-1} \text{H}_2$  for  $\text{Na}_2\text{Mg}_2\text{RuH}_8$ .

## Acknowledgements

We would like to acknowledge Ms. Warifune for the synthesis of the  $\text{Mg}_2\text{FeH}_6$  starting material. We also appreciate the financial support from JSPS KAKENHI Grant Number 25220911.

## Notes and references

- 1 K. Yvon and G. Renaudin, *Encyclopedia of Inorganic Chemistry*, John Wiley & Sons, Ltd, 2006.
- 2 K. Yvon, *Chimia*, 1998, **52**, 613–619.
- 3 J. J. Reilly and R. H. Wiswall, *Inorg. Chem.*, 1968, **7**, 2254–2256.
- 4 H. Blomqvist and D. Noréus, *J. Appl. Phys.*, 2002, **91**, 5141–5148.
- 5 M. Lelis, D. Milcius, E. Wirth, U. Halenius, L. Eriksson, K. Jansson, K. Kadir, J. Ruan, T. Sato, T. Yokosawa and D. Noréus, *J. Alloys Compd.*, 2010, **496**, 81–86.
- 6 R. J. Westerwaal, M. Slaman, C. P. Broedersz, D. M. Borsa, B. Dam, R. Griessen, A. Borgschulte, W. Lohstroh, B. Kooi, G. ten Brink, K. G. Tschersich and H. P. Fleischhauer, *J. Appl. Phys.*, 2006, **100**, 063518.
- 7 T. J. Richardson, J. L. Slack, R. D. Armitage, R. Kostecki, B. Farangis and M. D. Rubin, *Appl. Phys. Lett.*, 2001, **78**, 3047–3049.
- 8 M. Polanski, T. K. Nielsen, Y. Cerenius, J. Bystrzycki and T. R. Jensen, *Int. J. Hydrogen Energy*, 2010, **35**, 3578–3582.
- 9 M. Polanski, K. Witek, T. K. Nielsen, L. Jaroszewicz and J. Bystrzycki, *Int. J. Hydrogen Energy*, 2013, **38**, 2785–2789.
- 10 J. J. Didisheim, P. Zolliker, K. Yvon, P. Fischer, J. Schefer, M. Gubelmann and A. F. Williams, *Inorg. Chem.*, 1984, **23**, 1953–1957.
- 11 G. Li, M. Matsuo, S. Deledda, R. Sato, B. C. Hauback and S. Orimo, *Mater. Trans.*, 2013, **54**, 1532–1534.
- 12 T. J. Richardson, J. L. Slack, B. Farangis and M. D. Rubin, *Appl. Phys. Lett.*, 2002, **80**, 1349–1351.
- 13 B. Bogdanović, A. Reiser, K. Schlichte, B. Spliethoff and B. Tesche, *J. Alloys Compd.*, 2002, **345**, 77–89.
- 14 S. F. Parker, K. P. J. Williams, M. Bortz and K. Yvon, *Inorg. Chem.*, 1997, **36**, 5218–5221.
- 15 B. Huang, K. Yvon and P. Fischer, *J. Alloys Compd.*, 1995, **227**, 121–124.
- 16 B. Huang, F. Gingl, F. Fauth, A. Hewat and K. Yvon, *J. Alloys Compd.*, 1997, **248**, 13–17.
- 17 B. Huang, K. Yvon and P. Fischer, *J. Alloys Compd.*, 1994, **204**, 5–8.
- 18 G. Renaudin, L. Guenee and K. Yvon, *J. Alloys Compd.*, 2003, **350**, 145–150.
- 19 M. Orlova, J.-P. Rapin and K. Yvon, *Inorg. Chem.*, 2009, **48**, 5052–5054.



- 20 T. D. Humphries, S. Takagi, G. Li, M. Matsuo, T. Sato, M. H. Sørby, S. Deledda, B. C. Hauback and S. Orimo, *J. Alloys Compd.*, 2015, DOI: 10.1016/j.jallcom.2014.12.113.
- 21 M. Matsuo, H. Saitoh, A. Machida, R. Sato, S. Takagi, K. Miwa, T. Watanuki, Y. Katayama, K. Aoki and S. Orimo, *RSC Adv.*, 2013, **3**, 1013–1016.
- 22 H. Saitoh, S. Takagi, M. Matsuo, Y. Iijima, N. Endo, K. Aoki and S. Orimo, *APL Mater.*, 2014, **2**, 076103.
- 23 S. Takagi, T. D. Humphries, K. Miwa and S. Orimo, *Appl. Phys. Lett.*, 2014, **104**, 203901.
- 24 M. Di Chio, L. Schiffini, S. Enzo, G. Cocco and M. Baricco, *J. Alloys Compd.*, 2007, **434**, 734–737.
- 25 K. Kadir and D. Noréus, *Inorg. Chem.*, 2007, **46**, 3288–3289.
- 26 B. Huang, K. Yvon and P. Fischer, *J. Alloys Compd.*, 1992, **187**, 227–232.
- 27 B. Huang, K. Yvon and P. Fischer, *J. Alloys Compd.*, 1992, **190**, 65–68.
- 28 B. Huang, K. Yvon and P. Fischer, *J. Alloys Compd.*, 1993, **197**, 65–68.
- 29 J. A. Puszkiel, P. Arneodo Larochette and F. C. Gennari, *J. Alloys Compd.*, 2008, **463**, 134–142.
- 30 A. Boulitif and D. Louer, *J. Appl. Crystallogr.*, 2004, **37**, 724–731.
- 31 J. Laugier and B. Bochu, LMGP-Suite Suite Programs Interpret. X-ray Exp. by Jean laugier Bernard Bochu, ENSP/Laboratoire des Matériaux du Génie Phys. BP 46. 38042 Saint Martin d'Hères, Fr.
- 32 B. H. Toby, *J. Appl. Crystallogr.*, 2001, **34**, 210–213.
- 33 A. C. Larson and R. B. Von Dreele, *Los Alamos National Laboratory Report*, 2000, LAUR 86-748.
- 34 B. E. Warren, *X-ray Diffraction*, Courier Dover Publications, 1969.
- 35 H. Reardon, N. Mazur and D. H. Gregory, *Prog. Nat. Sci.*, 2013, **23**, 343–350.
- 36 D. A. Sheppard, M. Paskevicius and C. E. Buckley, *Chem. Mater.*, 2011, **23**, 4298–4300.
- 37 F. Bonhomme, K. Yvon, G. Triscone, K. Jansen, G. Auffermann, P. Müller, W. Bronger and P. Fischer, *J. Alloys Compd.*, 1992, **178**, 161–166.

